RESEARCH ARTICLE

Quantitative temporal proteomic analysis of human embryonic stem cell differentiation into oligodendrocyte progenitor cells

Raghothama Chaerkady[1,2], Brian Letzen[3*], Santosh Renuse[1,2,4], Nandini A. Sahasrabuddhe[1,2,5], Praveen Kumar[2], Angelo H. All[6], Nitish V. Thakor[6], Bernard Delanghe[7], John D. Gearhart[8], Akhilesh Pandey[1,9**] and Candace L. Kerr[3]*

[1] McKusick-Nathans Institute of Genetic Medicine and Department of Biological Chemistry, Johns Hopkins University School of Medicine, Baltimore, MD, USA
[2] Institute of Bioinformatics, International Technology Park, Bangalore, India
[3] Institute for Cell Engineering, Department of Obstetrics and Gynecology, Johns Hopkins University School of Medicine, Baltimore, MD, USA
[4] Amrita School of Biotechnology, Amrita Viswa Vidyapeetham, Kollam, Kerala, India
[5] Manipal University, Manipal, India
[6] Department of Biomedical Engineering, Johns Hopkins University School of Medicine, Baltimore, MD, USA
[7] Thermo Fisher Scientific (Bremen) GmbH, Bremen, Germany
[8] Institute for Regenerative Medicine, Department of Cell and Developmental Biology and Department of Animal Biology, University of Pennsylvania, Philadelphia, PA, USA
[9] Department of Pathology and Oncology, Johns Hopkins University School of Medicine, Baltimore, MD, USA

Received: February 25, 2011
Revised: June 19, 2011
Accepted: July 1, 2011

Oligodendrocytes (OLs) are glial cells of the central nervous system, which produce myelin. Cultured OLs provide immense therapeutic opportunities for treating a variety of neurological conditions. One of the most promising sources for such therapies is human embryonic stem cells (ESCs) as well as providing a model to study human OL development. For these purposes, an investigation of proteome level changes is critical for understanding the process of OL differentiation. In this report, an iTRAQ-based quantitative proteomic approach was used to study multiple steps during OL differentiation including neural progenitor cells, glial progenitor cells and oligodendrocyte progenitor cells (OPCs) compared to undifferentiated ESCs. Using a 1% false discovery rate cutoff, ~3145 proteins were quantitated and several demonstrated progressive stage-specific expression. Proteins such as transferrin, neural cell adhesion molecule 1, apolipoprotein E and wingless-related MMTV integration site 5A showed increased expression from the neural progenitor cell to the OPC stage. Several proteins that have demonstrated evidence or been suspected in OL maturation were also found upregulated in OPCs including fatty acid-binding protein 4, THBS1, bone morphogenetic protein 1, CRYAB, transferrin, tenascin C, COL3A1, TGFBI and EPB41L3. Thus, by providing the first extensive proteomic profiling of human ESC differentiation into OPCs, this study provides many novel proteins that are potentially involved in OL development.

Correspondence: Dr. Candace L. Kerr, Institute for Cell Engineering, Department of Obstetrics and Gynecology, Johns Hopkins School of Medicine, Baltimore, MD 21205, USA
E-mail: ckerr@jhmi.edu,ckerr2@jhmi.edu
Fax: +1-4109557427

Abbreviations: APOE, apolipoprotein E; **BMP1,** bone morphogenetic protein 1; **CLU,** clusterin; **EB,** embryoid body; **ESC,** embryonic stem cell; **FABP4,** fatty acid-binding protein 4; **FDR,** false discovery rate; **FGF,** fibroblast growth factor; **GPC,** glial progenitor cell; **ICC,** immunocytochemical; **LTQ,** linear trap quadrupole; **MARCKS,** myristoylated alanine-rich C-kinase substrate; **NCAM1,** neural cell adhesion molecule 1; **NID1,** nidogen 1 precursor; **NPC,** neural progenitor cell; **OCT4,** Octamer binding transcription factor 4; **OL,** oligodendrocyte; **OPC,** oligodendrocyte progenitor cell; **PDGF,** platelet-derived growth factor; **SBF1,** SET-binding factor 1; **SCX,** strong cation exchange; **SNAP23,** synaptosomal-associated protein, 23 kDa; **SOX,** sex determining region Y-box; **TNC,** tenascin C; **TNIK,** TRAF2 and NCK interacting kinase; **VIM,** vimetin; **WNT5A,** wingless-related MMTV integration site 5A

*These authors contributed equally to this work.
**Additional correspondence: Professor Akhilesh Pandey
E-mail: pandey@jhmi.edu
Colour Online: See the article online to view Figs. 1–5 in colour.

Keywords:
Biomedicine / Embryonic stem cell / iTRAQ / Oligodendrocyte / Pluripotency

1 Introduction

Oligodendrocytes (OLs) are central nervous system (CNS) glial cells that produce myelin, a multilamellar macromolecule that provides insulation to neuronal axons. Cultured OL lineage cells provide immense therapeutic opportunities for treating a variety of neurological conditions involving axonal demyelination. One of the most promising sources for such therapies is human embryonic stem cells (ESCs), which provide seemingly unlimited proliferation in vitro and are capable of differentiating into cells of all three germ layers. Moreover, ESCs are receptive to genetic manipulation and can therefore be optimized towards a particular therapeutic function. The use of human ESC-derived oligodendrocyte progenitor cells (OPCs) in rodent models of spinal cord injury and multiple sclerosis has been previously documented in the literature [1, 2]. Notably, the transplantation of human ESC-derived OPCs into the spinal cord of contused rats has been shown to promote partial recovery, which has led to the first Food and Drug Administration-approved human clinical trial involving cells derived from human ESCs.

The process of differentiation of pluripotent human ESCs is driven by an alteration of the gene expression program, which ultimately leads to formation of specific cell types. Identification of key factors involved in OPC-specific integration, multiplication and myelination can unveil new strategies for the treatment of a variety of afflictions affected by demyelination. Currently, known regulators of OL development include a multitude of signaling molecules, transcription factors and key metabolic pathways, which have been shown to control OL fate, proliferation, migration and survival [3, 4]. These molecules have been identified through a variety of methods that include in vitro culturing of OPCs with or without the presence of neurons [5], knockout rodent or chick electroporation studies, and by tissue characterization from patients with OL-affiliated diseases. Importantly, in vitro studies have revealed that cultured OLs produce myelin-associated lipids and proteins in a developmental timetable similar to that seen in vivo as well as demonstrating their ability to produce myelin-like sheaths. Using these approaches, a number of growth factors have been discovered, which promote OPC migration, survival and proliferation including platelet-derived growth factor (PDGF) [6, 7], fibroblast growth factor (FGF-2) [8, 9] and insulin-like growth factor-I [10]. In contrast to factors that support OPC proliferation, the thyroid hormone triiodothyronine (T3) [11], neuregulin-1 (NRG1) [12] and transforming growth factor-β (TGF-β1) were found to promote OL differentiation [13] along with FGF-2 when exposed to astrocytes [14]. The inductions of several transcription factors are also required for the maturation of post-mitotic OLs. These include oligodendrocyte transcription factor 1 and 2 (OLIG1, OLIG2), achaete-scute complex homolog 1 (ASCL1), NK2 homeobox 2 (NKX2.2), SRY (sex determining region Y)-box 10 (SOX10), Yin-Yang 1 transcription factor (YY1), myelin gene regulatory factor (MRF) and transcription factor 4 (TCF4) [15–18].

Despite the identification of several factors that appear to affect OPC proliferation and differentiation, little is known regarding factors regulating myelination or that initiate this process. While DNA microarray-based experiments have been carried out to identify such molecules, determining the protein expression using a quantitative proteomics approach is the most direct way to identify proteins that are specific to OL differentiation. To this end, we employed a high-throughput quantitative proteomics approach to systematically identify proteomic changes specific to OPC functions. We have previously successfully employed quantitative proteomic approaches to understand the differentiation of human ESCs into neurons and astrocytes [19]. Nanoflow LC combined with high-resolution Fourier transform MS methods allows for quantification of changes in low-abundance cellular proteins. In this report, using state-of-the-art MS analysis, expression profile analysis we have identified and quantified 3145 proteins at key stages of OL differentiation from human ESCs. In addition to generating a comprehensive proteomics database of OPC differentiation, the main objectives of this study were to characterize the progressive stage-specific expression of proteins with known or suspected roles leading to OL maturation and/or myelination and identify novel markers of various stages of OL development including neural progenitor cells (NPCs), glial progenitor cells (GPCs) and OPCs, utilizing a human ESC model of OL differentiation. Of significance, this approach characterizes intermediate time points during differentiation, including GPCs, which are not described in any other global expression profiling studies of the OL lineage.

2 Materials and methods

2.1 Cell culture

H1 (WA01) human ESCs were purchased from WiCell (Madison, WI) and expanded on irradiated mouse embryonic fibroblasts in ESC growth media, consisting of DMEM/F12, 20% KnockOut serum (Invitrogen), 2 mM glutamax, 2 mM nonessential amino acids and 3.5 μL β-mercaptoethanol supplemented with basic FGF-2. Prior to differentiation, ESCs were dispersed using 0.05% trypsin/EDTA and plated on matrigel (BD Bioscience) for 5 days with feeder-conditioned media. Cells were then differentiated

into embryoid bodies [20], NPCs, GPCs and OPCs, according to previously published protocols [21, 22].

Briefly, neural differentiation of ESCs was initiated via embryoid body (EB) suspensions with N2B27 medium supplemented with 200 ng/mL noggin, 20 ng/mL FGF-2 and 20 ng/mL FGF-4 (R&D Systems). Neural EBs were grown for 15 days and then plated onto matrigel and grown in N2B27 media supplemented with 20 ng/mL FGF-2 for 5 days to produce nestin+/A2B5+NPC, capable of deriving cells with neuronal and glial fates. Next, 20 ng/mL Epidermal growth factor (EGF) (PeproTech) was added to produce Platelet-derived growth factor receptor (PDGFR)-α+/Olig1 +GPC, which can differentiate into either astrocytes or OLs. To promote differentiation into OPCs, the medium was supplemented with 20 ng/mL PDGF-AA (R&D Systems). After 25 days, OPCs were identified by O1, O4, GalC and CNPase expression. Samples for proteomic analysis were isolated from four distinct cell stages: ESC, NPC, GPC and OPC. For these stages, immunocytochemical (ICC) analysis was performed on co-cultures to confirm >95% purity in the expression of markers discussed above.

2.2 ICC analysis

Immunocytochemistry was carried out on EBs, NPCs, GPCs and OPCs with primary antibodies listed in Supporting Information Table 1 using standard protocols and fluorescent secondary antibodies (Millipore). The cells were frozen in Octamer binding transcription factor 4 (OCT4) freezing compound (TissueTek), sliced into 5 µm sections and positioned on slides (ProbeOn Plus, Fisher Scientific). DAPI was used for nucleus staining to determine the percentage of immunopositive cells.

2.3 Cell lysates, in-solution digestion and iTRAQ labeling

Four different cell stages generated in duplicate (in total of eight cell culture plates) were pooled and selected for proteomic analysis (Fig. 1). ESCs, NPCs, GPCs and OPCs were washed with ice cold phosphate buffered saline six times to completely remove the traces of serum proteins. The cells were lysed by sonication in 0.5% SDS for 20 s on ice (Duty cycle 40%, output control at 4, on Sonifier 250, Branson) three times at 5 min intervals. Equal amount of proteins from each cell type based on protein estimation (Lowry's method) were used for 4-plex iTRAQ (Applied Biosystems, Cat. No. 4352135) labeling according to manufacturer's protocol unless otherwise noted [23]. Briefly, 80 µg proteins from each cell type was reduced using 2 µL of tris(2-carboxyethyl) phosphine at 60°C for 1 h and cysteine residues were alkylated with 1 µL of methyl methanethiosulfonate for 10 min at room temperature. The samples were diluted in 50 mM triethylamonium bicarbonate to dilute the SDS concentration to 0.02%. The samples were then digested using sequencing grade trypsin (Promega) (1:20) for 12 h at 37°C. The volume of digestion mixture was reduced by vacuum drying and peptides from each sample in a final volume of 35 µL was incubated with one of the four iTRAQ reagents diluted in 70 µL of absolute ethanol (200 proof) at room temperature. The peptides from ESCs, NPCs, GPCs and OPCs were labeled using iTRAQ reagents containing 114, 115, 116 and 117 reporter ions, respectively. After 2 h, 100 µL water was added to each iTRAQ labeling reaction mixture and the samples were vacuum dried to ~40 µL to remove excess of triethyl ammonium bicarbonate and ethanol. The samples were subsequently combined and diluted to 1 mL in 5 mM potassium phosphate buffer (pH 2.7) containing 30% acetonitrile (Solvent A). The pH of the sample was adjusted to 2.7 using 100 mM phosphoric acid. The iTRAQ labeled peptides were fractionated using strong cation exchange (SCX) chromatography using polysulfoethyl A column (PolyLC, Columbia, MD) (300 Å, 5 µm, 100 × 2.1 mm) [24] on an Agilent 1100 HPLC system consisting of a binary pump, external sample injector, UV detector and a fraction collector. Fractionation was carried out for a period of 45 min using a linear gradient of increasing salt concentration of up to 350 mM KCl in solvent A. The fractions were pooled to generate 14 fractions and dried in vacuum dryer. The samples were reconstituted in 40 µL of 0.1% trifluoroacetic acid and desalted using homemade C_{18} (3 M Empore high-performance extraction disks) stage-tips in 200 µL pipette tips. The samples were split into two sets, one was analyzed on linear trap quadrupole (LTQ)-Orbitrap XL and other was analyzed on LTQ-Orbitrap Velos.

2.4 LC-MS/MS

Nanoflow electrospray ionization LC-MS/MS analysis of the first set of iTRAQ labeled samples was carried out on an LTQ Orbitrap XL (Thermo Scientific) interfaced with reversed phase system controlled by Eksigent nano-LC and Agilent 1100 microwell plate autosampler. The second set was analyzed as a technical replicate using LTQ Orbitrap Velos (Thermo Scientific) mass spectrometer. The desalted SCX fractions were rapidly enriched (5 µL/min) on a trap column (75 µm × 2 cm, Magic C_{18}AQ Michrom Bioresources, 5 µm, 100 Å) and separated on an analytical column (75 µm × 10 cm, Magic C_{18}AQ Michrom Bioresources, 5 µm, 100 Å) with a nanoflow solvent delivery. The MS and MS/MS data were acquired at a resolution of 60 000 at *m/z* 400 and 7500 at *m/z* 400, respectively. For each cycle of data-dependent analysis, ten and 20 most abundant peptides were selected for MS/MS analysis in LTQ Orbitrap XL (normalized collision energy 37%) and LTQ Orbitrap Velos (normalized collision energy 40%), respectively. Higher collision dissociation mode was used for MS/MS scans. Two-stepped collision energy with a width of 6% was used to cover the best fragmentation event in which two

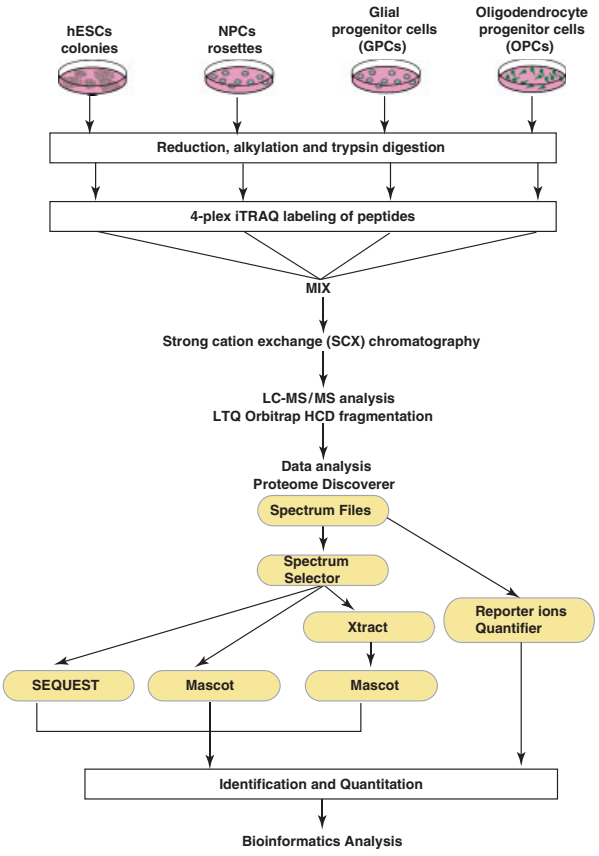

Figure 1. Outline of the 4-plex iTRAQ-based quantitative proteomic strategy. iTRAQ labeling was carried out using lysates from ESCs, NPCs, GPCs and OPCs. Samples were digested using trypsin and labeled using iTRAQ reagents 114, 115, 116 and 117 with peptides from ESCs, NPCs, GPCs and OPCs, respectively. After labeling, peptides from all four samples were combined and fractionated by SCX chromatography. Each fraction was then analyzed by LC-MS/MS on an LTQ Orbitrap mass spectrometers. The data were analyzed using Proteome Discoverer software.

normalized collision energies around the set CEs were applied to fragment the peptides.

2.5 MS data analysis

The MS data were processed using Proteome Discoverer (Version 1.2.0.208) software (Thermo Scientific) workflow. The Proteome Discoverer workflow consisted of spectrum selector and reporter ion quantifier including MASCOT and Sequest search nodes (Fig. 1). MS/MS spectral data were also processed using extract feature of Proteome discoverer under MASCOT search component of the workflow. For both nodes, the same search parameters were selected, which include iTRAQ label at tyrosine, oxidation of methionine, deamidation at NQ as variable modifications. iTRAQ label at N-terminus and lysine, methylthio label at cysteine were used as fixed modifications. The MS data were searched against NCBI RefSeq 40 human protein database containing 31 811 sequences. Using proteome discoverer workflow, the data from MASCOT and Sequest search nodes were merged to obtain average quantitation values from replicates. False discovery rate (FDR) for peptide search is a statistical value that determines the number of false identifications among all identifications. Proteome Discoverer calculates the percentage of false identifications using a separate decoy database (reverse database) that contains the reversed sequences of the protein entries. An FDR threshold of 1% was used in this study. The software counts the number of matches from both searches and calculates the FDR by counting only the top match per spectrum assuming that only one peptide can be the correct match. The score thresholds are adjusted to obtain 1% reversed hits compared to forward hits. MASCOT significant threshold based on peptide score was used as filter settings for FDR calculation in MASCOT searches and Xcorr versus charge state for filter settings in Sequest searches. Precursor and reporter ion window tolerance were fixed at 20 ppm and 0.05 Da, respectively. The criteria specified for generation of peak lists include signal to noise ratio of 1.5 and inclusion of precursor mass range of 600–8000 Da. Proteome Discoverer software performs automated statistical analysis of the results and uses unique peptides to calculate accurate relative protein quantitation. The peptide and protein data were extracted using high peptide confidence and top one peptide rank filters. FDR was calculated by enabling the peptide sequence analysis using decoy database. The average ratio and percentage variability was used for protein quantitation wherever multiple peptides were identified for a protein.

2.6 Data analysis

Technical and biological replicates were used for MS analysis and ICC analysis of differentiation, respectively. The proteins derived from search results were filtered by using a criterion of >2.0-fold change relative to the undifferentiated ESCs. Proteins that did not exhibit this cutoff for at least one stage were removed from the analysis. DAVID (database for annotation, visualization and integrated discovery) analysis tool was used to categorize proteins from the data set into functional groups and cellular localizations [25, 26]. Differentially expressed proteins were ranked to produce lists of the top 50 upregulated proteins at each stage of differentiation (NPCs, GPCs and OPCs). To identify upregulated proteins associated with myelination, a custom algorithm was developed within MATLAB (Mathworks, Natick, MA) to conduct an automated Pubmed literature search for each protein along with the keyword "myelin". The algorithm returned the number of "hits" for each protein, and those returning at least one result were manually evaluated for known or predicted roles in

myelination. To identify potential novel markers of NPCs, GPCs and OPCs, proteins were selected, which demonstrated significant upregulation (>2.0-fold change) in only one of these stages and relatively flat expression (<1.0-fold change) across all other stages.

3 Results

3.1 ESC differentiation into OL lineage cells

The differentiation protocol for the generation of NPCs, GPCs and OPCs from human ESCs is shown in Supporting Information Fig. 1A [21, 22]. These stages were characterized by changes in morphology and immunofluorescent marker expression after alteration of substrate adherence conditions and growth factors. Supporting Information Fig. 1B shows immunofluorescent marker staining in NPCs, GPCs and OPCs throughout differentiation. These images were produced from cocultures and exhibited >95% purity of relevant immunofluorescent markers. Pluripotent ES cells showed morphological integrity along with expression of OCT4 and alkaline phosphatase. After ES cells were suspended in N2B [27] media for 15 days, neural EB cells formed, which expressed NESTIN, PAX6 and SOX1. Conversely, the expression of pluripotent markers diminished as differentiation progressed. NPC demonstrated a flattened morphology and expressed Sox10 and A2B5 after reattachment to matrigel for 5 days. Upon the introduction of EGF, the neural progenitors produced GPCs, which expressed PDGFR-α, NG2 and Olig1 and demonstrated a bipolar morphology. In response to PDGF-AA, OL progenitors formed, which progressively expressed O4, O1, GalC and CNPase markers [20–26]. OPCs also developed multiple filopodial extensions. OPC samples used for proteomic analysis continued to proliferate in culture and did not express myelin basic protein, which is the most common marker of mature OLs.

3.2 LC-MS/MS analysis of iTRAQ-labeled peptides

From replicate analyses, nearly 22 200 peptides (~13 887 unique peptides, 1728 protein groups) were identified from samples analyzed on LTQ-Orbitrap XL and ~58 900 peptides (~37 440 unique peptides, 2956 protein groups) were identified from samples analyzed on LTQ-Orbitrap Velos; Supporting Information Fig. 2. By merging MASCOT and Sequest search results of data obtained from LTQ-Orbitrap XL and LTQ-Orbitrap Velos, we obtained 3145 unique proteins (5230 proteins before grouping) at a 1% FDR cutoff. This list also includes ~100 proteins whose iTRAQ ratio was not determined because of low reporter signal. A complete list of proteins identified in all the analyses is shown in Supporting Information Table 2. When peptides were identified with 1% FDR but the iTRAQ reporter levels were too low for quantitation fold changes peptides were appropriately ascribed as either ''Not Determined'' because of low iTRAQ reporter signal or as ''Variability is Not Applicable'' if there was only a single data point. In a similar fashion, the details of proteomic analysis including sequence coverage, number of unique peptides, quantitation results with percentage variability are included in the list. A list of all non-redundant peptides identified in this study is given in Supporting Information Table 3.

Different expression patterns were observed based on quantitative proteomics data from four different cell stages. MS/MS and iTRAQ reporter ion spectra of representative peptides from proteins with different expression levels in ESCs, NPCs, GPCs and OPCs are shown in Fig. 2. Panel A shows the MS/MS spectrum of a peptide from β actin with similar levels of intensity of the reporter ions. Panel B shows the MS/MS spectrum and reporter ions of a peptide from podocalyxin-like isoform 1, a known pluripotency marker, which was downregulated during differentiation process. Panel C shows high expression of CD44 in NPCs and panel D shows expression of synaptopodin A in all cell stages except in ESCs. Panels E and F show high expression of clusterin (CLU) 1 and integrin α 1 in GPCs and OPCs, respectively. Panels G–I show examples of proteins (myristoylated alanine-rich C kinase, apolipoprotein E (APOE) and transferrin (TF)) with progressive increase in expression during OPC formation from ESCs. Panels J–L show examples of proteins (fatty acid binding protein 4 (FABP4), α crystallin B and neural cell adhesion molecule 1), which showed highest level of expression in OPCs compared to ESCs, NPCs and GPCs). Overall, among 3140 proteins, only 80 proteins including OCT4 and SP3 were excluded from quantitation due to the poor intensity of reporter ions. Nearly 7.4 % of the proteins showed more than twofold upregulation and 6.5% of the proteins showed downregulation in OPCs when compared to ESCs. Figure 3A shows graphical distribution of iTRAQ ratios of all the quantitated proteins and differential expression of a small subset of proteins from OPCs. The majority of proteins (86%) showed no significant change in abundance levels. Individually, NPCs, GPCs and OPCs showed 5.2, 3.7 and 7.4% upregulated proteins when compared to ESCs, respectively. Similarly, NPCs, GPCs and OPCs showed 2.9, 3.5 and 6.5% downregulated proteins when compared to ESCs, respectively. Samples used for iTRAQ experiments were normalized by averaging iTRAQ fold changes of peptides from actin α2 for each stage. Results include ~1650 peptide-spectrum matches from 22 peptides (Fig. 3B).

3.3 Differentially expressed proteins

Proteins with more than twofold increase in abundance as compared to ES cells were classified as differentially upregulated, and those with abundance ratios of 0.5-fold or less as compared to ES cells were classified as differentially downregulated. Supporting Information Table 4 shows the

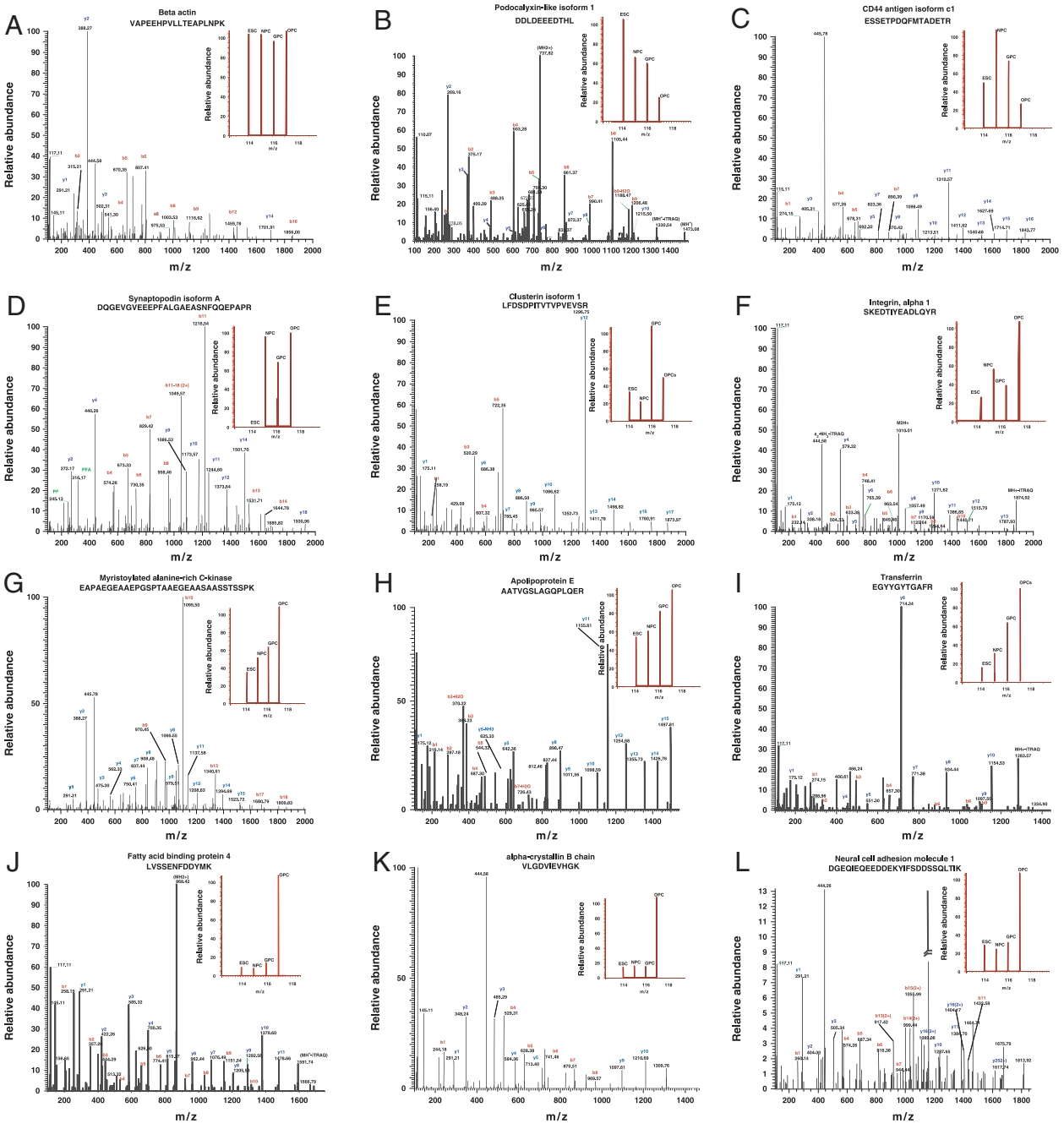

Figure 2. Representative MS/MS spectra of iTRAQ-labeled peptides from selected proteins. (A) No change in iTRAQ fold change (β actin); (B) High in ESCs (podocalyxin-like isoform 1); (C), High in NPCs (CD44); (D), High in NPCs, GPCs and OPCs (synaptopodin A); and (E) and (F), high expression of CLU 1 and integrin α 1 in GPCs and OPCs respectively. (G–I) Progressive increased expression during OPC formation from ESCs (myristoylated alanine rich C kinase, APOE and TF, respectively). (J–L) Highest level of expression in OPCs compared to ESCs, NPCs and GPCs (FABP4, α crystallin B and NCAM1, respectively).

list of proteins significantly overexpressed (≥2.0-fold) in at least one stage such as NPCs, GPCs or OPCs when compared to ESCs. Similarly, Supporting Information Table 5 shows the list of proteins underexpressed (≤0.5-fold) at least in one stage such as NPCs, GPCs or OPCs when compared to ESCs. In ESCs, 272 proteins showed high expression compared to NPCs, GPCs or OPCs and 344 proteins showed lower expression in ESCs compared to at least one cell stage. Similarly, 159 proteins showed upregulation in NPCs compared to ES cells, while 90 showed downregulation. The highest upregulated protein (>30-fold) at this stage was early endosome antigen 1 (EEA1). The

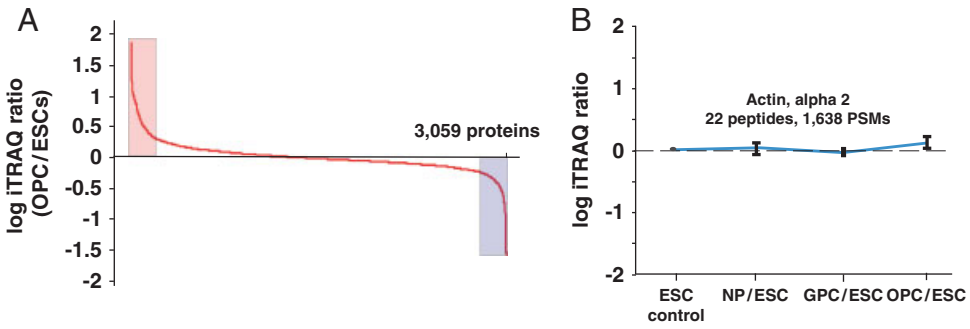

Figure 3. The distribution of iTRAQ fold changes. (A) Protein expression levels observed in ESCs and OPCs. (B) Average ratios of expression of actin α 2 in four different cell stages calculated using ~1650 peptide-spectrum matches.

GPC stage showed 113 upregulated proteins and 107 downregulated proteins. At GPC stage krueppel-like factor 16 (KLF16) was highly expressed (>12-fold increase) when compared to ESCs. Cells at the OPC stage contained the greatest differential expression relative to ESCs, with 223 upregulated proteins and 198 downregulated proteins. In both GPCs and OPCs, prenylcysteine oxidase-like (PCYOX1L) matrix metalloproteinase 9 (MMP9), COP9 constitutive photomorphogenic homolog subunit 2 isoform 1 (COPS2) showed more than 12-fold upregulation when compared to ESCs. The most highly expressed protein at GPC stage includes high mobility group protein HMGI-C isoform a, β-crystallin B3, hypothetical protein encoded by *C6orf211*, α 2 type IV collagen (with a fold-change of >15). Therefore, this data set is the first comprehensive report of the earliest differences in protein expression seen during glial differentiation from ESCs.

Several pluripotency markers including PODXL, LIN28A, LIN28B, TRIM28, LEFTY2 showed decreased expression levels during differentiation (≤0.5-fold in at least one stage, Supporting Information Table 5). Due to increased sensitivity and high-resolution MS, we were able to identify many transcription factors expressed in ESCs. The levels of many of the proteins involved in transcription regulation (SP1, CHAF1B, DNMT3A, EHMT1, JARID2, MYBBP1A, NFXL1, ORC2, PAWR, SQSTM1 and TIAL1) were found to be decreased during ESC differentiation (≤0.5-fold in at least one stage, Supporting Information Table 5).

Functional analysis of the protein data set using database for annotation, visualization and integrated discovery [27] tool revealed differential regulation of important classes of proteins in ESCs, NPCs, GPCs and OPCs. Table 1 categorizes proteins predominately expressed at each stage, which are associated with transcriptional regulation, plasma membrane proteins, proteins implicated in cell differentiation, cell signaling, and cell adhesion.

3.4 Differentially expressed proteins in OPCs

As expected, cells at the OPC stage contained the greatest number (26) of differentially expressed proteins with known or suggested roles in myelination. A large majority of these proteins (88%) demonstrated the greatest upregulation at the OPC stage, including neural cell adhesion molecule 1 (NCAM1), APOE, tenascin C (TNC), vimentin (VIM), wingless-related MMTV integration site 5A (WNT5A), and heat shock 27 kDa protein 1 among several others. NCAM1 is a cell adhesion molecule found in both neurons and OLs, which has been suspected to be involved in axon-OL signaling during myelination. Upregulation of NCAM1 in cultured OPCs was found to promote radial process outgrowth [28]. Our results show that protein levels increased as ES cells differentiated into OPCs, concomitant with increased outgrowth of radial processes. Similarly, brain acid-soluble protein (BASP1) has also been shown to promote neurite outgrowth [29] and in our data increased throughout differentiation, suggesting a role in OL process development. Additionally, a group of crystallins (CRYAA, CRYAB, CRYBA1 and CRYBB) showed significantly higher expression in OPCs compared to other stages (Fig. 2, panel K). Recently CRYAB has been shown to specifically accumulate in OLs [30] CRYAB, an inhibitor of inflammation, has been shown to demonstrate anti-apoptotic and neuroprotective roles in the CNS [31]. Finally, APOE also demonstrated progressive increase during OPC differentiation (Fig. 2, panel H). Myristoylated alanine-rich C-kinase substrate (MARCKS) is an actin filament crosslinking protein, which plays a role in vesicular trafficking to the myelin sheet in mature OLs. The regulation of PI(4,5)P2 by MARCKS has been suggested to play a role in the outgrowth of membranous cellular processes in mature OLs [32]. Previous studies have found that MARCKS mRNA levels increase as OLs mature, suggesting developmental regulation of this protein [33]. However, there is limited information in the literature regarding the protein expression of MARCKS along OL differentiation. Our protein data show progressive upregulation of MARCKS in developing OLs (Fig. 2, panel G), in agreement with mRNA data. In addition, bone morphogenetic protein 1 (BMP1), which has been shown to play an important role in OL development, demonstrated significant upregulation. Interestingly, reduction of endogenous BMP1 expression in developing glial cells has been shown to reduce maturation of OLs and myelin protein expression, without affecting OPC numbers [34]. These data are

Table 1. List of proteins from specific classes overexpressed in ESCs, NPCs, GPCs and OPCs based on their relative abundance in each cell stage

	Regulation of transcription	Plasma membrane	Differentiation/ morphogenesis	Intracellular signaling	Cell adhesion and junction
ESCs	CHAF1B	ALDH3A2	CASP3	RAB3B	CAV1
	DNMT3A	ANK3	EZR	CAV1	CDH1
	EHMT1	APOA1	KRT5	APOA1	CGN
	JARID2	CASP3	DSP	SQSTM1	CLDN6
	MYBBP1A	CAV1	KRT2	RRAS2	CXADR
	NFXL1	CDH1	SEMA6A	TAB1	DMXL2
	ORC2	CLDN6	TUBB2A	UBE2C	DSG2
	PAWR	CLDN7	ANK3	SRPK1	DSP
	SP1	CXADR	GJA1	METAP2	GJA1
	SQSTM1	DMXL2	CDH1	SPINT2	HLA-A
	TIAL1	EPCAM			HLA-C
		EZR			LCP1
		GJA1			OCLN
		HLA-A			PKP2
		IFITM1			UBAP2
		KRT1			VCL
		OCLN			
		PAWR			
		PODXL			
		RAB3B			
		SLC2A1			
		SLC3A2			
		SLC7A5			
		SPINT2			
		STXBP2			
		TAGLN2			
		TNFRSF8			
		VCL			
NPCs	CAND1	ACTR2	AMBRA1	ARHGEF2	ARHGAP17
	CREB1	AMFR	CD44	ITGA1	ARHGEF2
	EP300	CD44	CREB1	MED14	CD44
	HMGA2	CTNNA2	CTNNA2	PKN1	COL11A1
	HUWE1	EXOC8	DBN1	RHEB	COL3A1
	KLF16	GYPC	DPYSL5	RNF14	CTNNA2
	MCTS1	ITGA1	GPSM1	SOD1	ITGA1
	MED14	NT5E	HUWE1	TGM2	LMO7
	RCOR2	PALM	ITGA1	TNIK	SNAP23
	RFX3	PON2	SOD1		SYNPO
	RNF14	RFTN1	SOX2		
	RRP8	RHEB	VPS33A		
	SETD1A	SBF1			
	SIN3A	SNAP23			
	SOX2				
	WHSC1L1				
	ZSCAN18				
GPCs	ARHGEF10L	ACTR2	AGRN	AGRN	ARHGAP17
	AGRN	AGRN	ATXN10	AXL	CTNNA2
	ARID3A	CAPRIN1	CLU	CREB1	LAMA1
	BTAF1	CTNNA2	CREB1	KLF16	LAMB1
	CAND1	HSPG2	CTNNA2	LAMA1	
	CAT	NT5E	LAMB1	MAP2K1	
	CREB1	PON2	MAP2K1	MED14	
	HMGA2	RFTN1	MMP9	MINK1	
	HUWE1	RHEB	VPS33A	MMP9	
	KLF16	SBF1		OXSR1	
	MCTS1	SLC2A6		RFC4	

Table 1. Continued

	Regulation of transcription	Plasma membrane	Differentiation/ morphogenesis	Intracellular signaling	Cell adhesion and junction
	MED14	SNAP23		RHEB	
	RCOR2	SPAG9		SPAG9	
	RFX3				
	RSF1				
OPCs	AGRN	ACTR2	AGRN	AGRN	BMP1
	ARHGEF10L	AGRN	APOE	APOE	COL12A1
	CAND1	AMFR	ATXN10	COL3A1	COL3A1
	CAT	BASP1	CRYAA	CRYAB	COL5A1
	CRABP2	CCDC8	DBN1	DBNL	COL6A1
	FABP4	CRIP2	FN1	GNG2	COL6A3
	HMGA2	EPB41L3	ITGA1	GSN	EMILIN1
	HUWE1	FN1	MMP9	ITGA1	FN1
	KLF16	GNG2	NEFL	KLF16	HSPG2
	LBH	GPC6	NEFL	NCAM1	ITGA1
	LBH	HSPG2	RELA	OXSR1	LMO7
	LMCD1	ITGA1	SFXN1	PRKACA	MFGE8
	PBXIP1	MARCKS	TF	PRKAR2A	NCAM1
	PBXIP1	MRC2	VPS33A	TGM2	POSTN
	RELA	NCAM1		THBS1	SCARB2
	SMARCD3	NT5E		WNT5A	TGFBI
	TCEA3	PALM			THBS1
	WHSC1L1	PON2			TNC
	ZNF512B	PON2			
		RFTN1			
		SBF1			
		SCARB2			
		SLC2A6			
		SNAP23			

consistent with the increasing endogenous expression of BMP1 in our cultured OPCs, serving to promote later OL maturation. Recent studies in the peripheral nervous system have shown that an APOE-mimetic peptide significantly improved axon elongation, myelin debris clearance and remyelination after crush injury [35].

3.5 Myelination-associated proteins

Next, we compiled an expanded list of proteins shown by previous studies to have either a known or putative role in OL myelinating potential. This was accomplished via a custom script we developed to perform an automated Pubmed literature search for each protein along with the keyword ''myelin''. Proteins that generated one or more hits via this method were manually verified for associated roles in myelination. For this purpose, proteins that showed >2-fold upregulation at the NPC, GPC, and OPC stages relative to the ESC stage were selected for analysis. Figure 4 presents the temporal expression pattern of potential ''myelin-potentiating'' proteins showing differential expression at the NPC stage (panel A), GPC stage (panel B) and OPC stage (panel C). Three of these proteins (synaptosomal-associated protein, 23 kDa (SNAP23), SET-binding factor 1 (SBF1) and TF) were differentially expressed at all three stages. SNAP23, which plays a role in membrane fusion during intracellular trafficking, demonstrated peak expression at the neural progenitor stage and showed high but decreased expression at the GPC and OPC stages. SBF1 was found to decrease as NPCs differentiated into GPCs and then increase upon OPC differentiation. SBF1 is a pseudophosphatase homolog to MTMR13, which has been shown to be associated with demyelination when mutations are present in this gene [36]. Finally, our data for TF show progressively increased expression throughout OL differentiation, aligned with a report by Espinosa-Jeffrey et al. discussing stage-dependent expression of TF (Fig. 2, panel I) [37].

Interestingly, NPCs and GPCs expressed a similar number of differentially expressed proteins that have been associated with glial development. We found nine such proteins to be significantly upregulated in NPCs and GPCs, which decreased as these cells differentiated into OPCs. Most of these proteins have been associated with astrocyte development. These proteins included CD44 molecule (CD44), superoxide dismutase 1, SNAP23, TRAF2 and NCK interacting kinase (TNIK). Proteins with highest expression at the

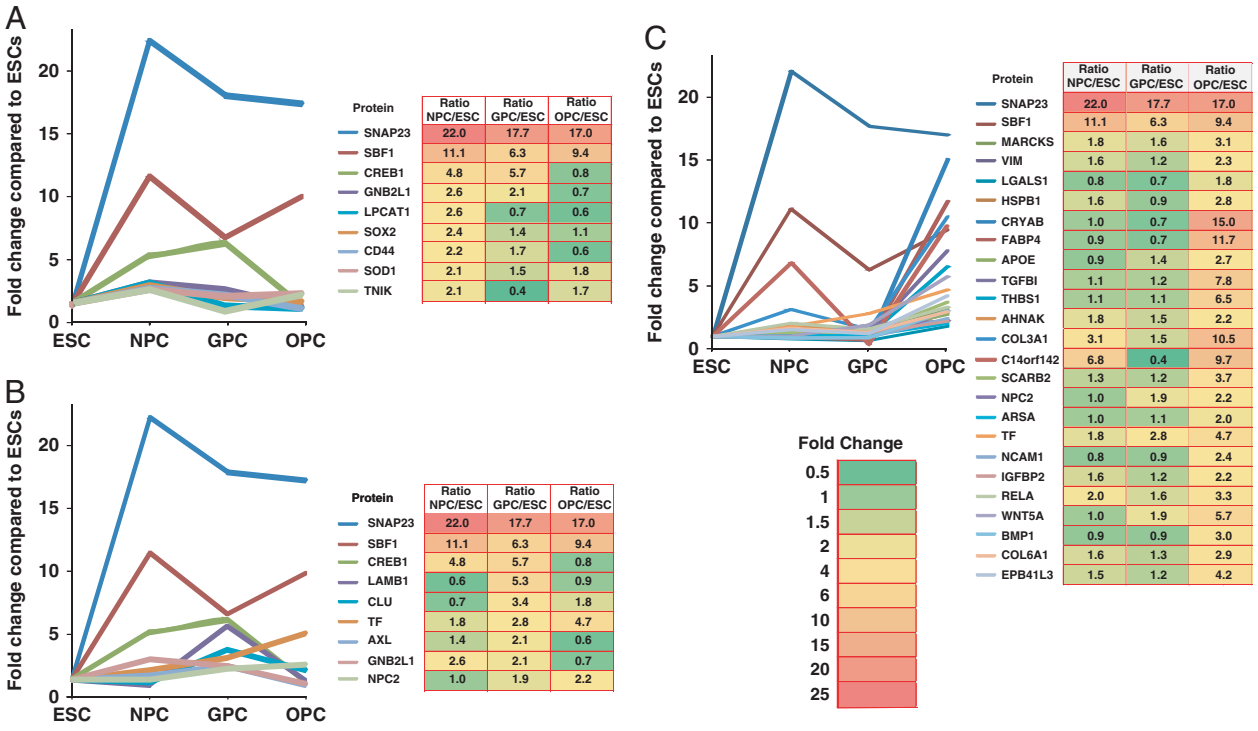

Figure 4. Stage-specific expression profiles of differentially expressed proteins with known or suspected roles in myelination. (A) Upregulated proteins especially in NPCs. (B) Upregulated proteins especially in GPCs. (C) Upregulated proteins in OPCs.

GPC stage included CLU, AXL receptor tyrosine kinase (AXL), cAMP responsive element binding protein 1 (CREB1) and laminin β 1. CLU levels were found to significantly decrease from the GPC to OPC stages. This protein has been shown to be expressed in astrocytes but not in OLs [38, 39]. Accordingly, the dramatic decrease in expression within our data may be concomitant with the inhibition of astrocyte differentiation and the promotion of OL differentiation.

3.6 ICC validation of differentially expressed proteins

Changes in protein levels were validated using ICC staining for several potential regulators of OL maturation. Levels of staining were compared in neural progenitors, glial progenitors and in OL progenitors, which corroborated the proteomic data. WNT5A, MARCKS, APOE, CRYAB and VIM showed increased levels of staining from NPC to OPC while superoxide dismutase 1, SNAP23, and the stem cell marker HMGA1 showed a decline in expression during OPC development (Fig. 5). Trends similar to the proteomic data were also demonstrated for CLU and TNIK where CLU demonstrated highest expression and TNIK lowest expression in GPCs compared to NPCs and OPCs.

4 Discussion

Significant discoveries have been made in the past two decades regarding OL development and their roles in disease progression [40–42]. These studies have included transgenics and knock-out models that have independently demonstrated roles for many growth factors or transcription factors in OL maturation and function (for review see [43]). However, a clearer understanding of the pathways involved in their regulation and their potential interactions necessitates further investigation. In attempts to identify pathways and their interactions, several global gene expression studies of OL lineage cells have been described. For instance, Lin et al. and Hu et al. utilized global expression profiling to compare differences in gene expression patterns between OLs derived at various developmental ages [44, 45], and Kippert et al. analyzed gene expression of OLs derived from a mouse oligodendroglial cell line, Oli-neu [46]. While these studies provide valuable information and successfully characterized the comprehensive expression of mRNA within these samples, it is difficult to make any firm conclusions concerning the true protein levels. It is well known that posttranscriptional mechanisms such as miRNA regulation commonly account for discrepancies between observed mRNA and protein levels, thus emphasizing the importance of measuring protein levels for a direct indication of ultimate gene expression.

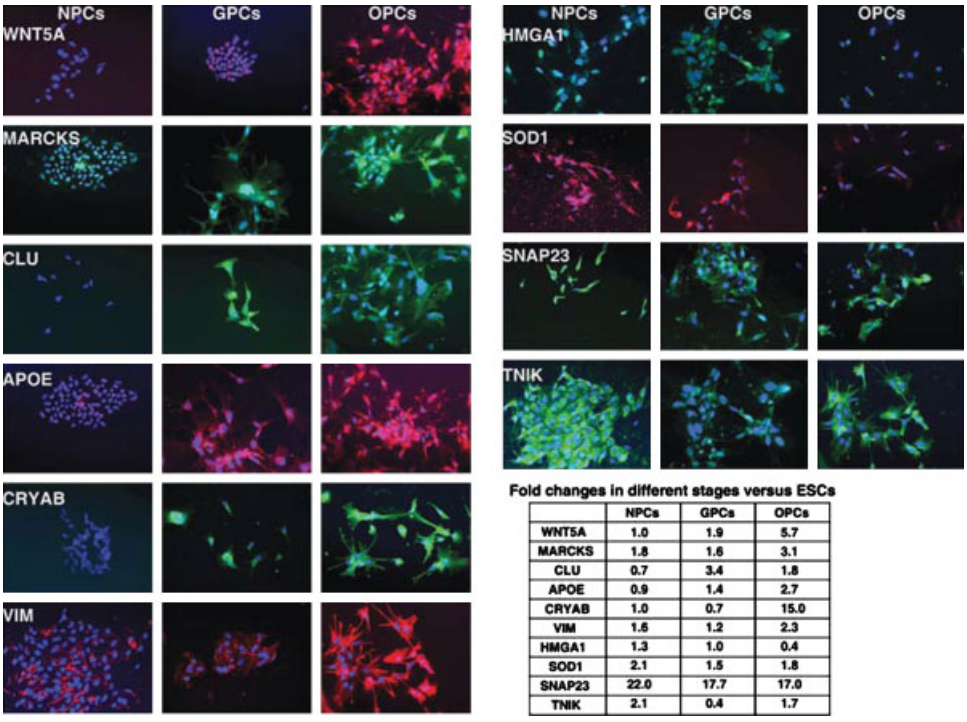

Fold changes in different stages versus ESCs

	NPCs	GPCs	OPCs
WNT5A	1.0	1.9	5.7
MARCKS	1.8	1.8	3.1
CLU	0.7	3.4	1.8
APOE	0.9	1.4	2.7
CRYAB	1.0	0.7	15.0
VIM	1.6	1.2	2.3
HMGA1	1.3	1.0	0.4
SOD1	2.1	1.5	1.8
SNAP23	22.0	17.7	17.0
TNIK	2.1	0.4	1.7

Figure 5. ICC validation of proteins expressed in NPCs, GPCs and OPCs. Semi-quantitative immunofluorescence analysis in NPCs, GPCs and OPCs. Images were generated with similar exposure times to compare staining intensity of different stages. DAPI (blue) used as a nuclear stain.

Nonetheless, several of the genes identified in these rodent models were also found in our proteomic analyses. For instance, TF, NCAM1, APOE, FABP4, TNC, WNT5A, GDI1 and TGFBI showed consistently increased expression as NPCs differentiated into OPCs. As might be expected from these myelin or OL lineage associated proteins, the majority of these experienced the highest upregulation at the final GPC to OPC stage transition. Interestingly, our previous neuronal proteomics study showed extensive downregulation of APOE in motor neurons and moderate downregulation in astrocytes. Similarly, TNCs showed higher expression in astrocytes than in motor neurons. Together, these expression patterns are consistent with the potential role of TNCs and APOE into glial fate. In contrast, CD44 showed consistent downregulation along differentiation from NPCs to OPCs. CD44 is normally found in astrocytes and microglia and is expressed only during pathological conditions within OLs [47]. Hence, decreased expression of CD44 may be vital for directing neural progenitors into the oligodendroglial fate and away from astrocyte differentiation. In addition, several proteins that have been characterized during OL development demonstrated a unique intermediate pattern of expression in GPCs compared to NPCs and OPCs. For instance, VIM, SBF1, AHNAK, ACAT2, MAP1A, TNIK, insulin-like growth factor BP2, heat shock 27 kDa protein 1 and CRYAB expression decreased from NPCs to GPCs followed by an upregulation in OPCs. Interestingly, these trends were unique for OPC differentiation compared to our previous study of neuronal proteomic profiling, where these proteins demonstrated either a consistent increased or decreased expression during NPC differentiation into HB9 expressing motor neurons.

While the focus of this study was to characterize the developmental stage-specific expression of proteins with known or suspected roles in myelination, another objective was to identify potential novel markers of NPCs, GPCs and OPCs. For example, two proteins were specifically expressed at the NPC stage, including methyl-CpG binding domain protein 3 and activating molecule in beclin-1-regulated autophagy (AMBRA1). Methyl-CpG binding domain protein 3 is involved in histone deacetylation and has been shown to decrease pluripotency by repressing OCT4 in cooperation with CDK2AP1 [48]. As such, its expression in NPCs may be associated with repressing pluripotency and encouraging differentiation. Additionally, the GPC stage resulted in a higher number of potential markers, including pleckstrin homology domain containing, family A member 5 isoform 2 (PLEKHA5), laminin β 1 precursor (LAMB1), laminin α 1 precursor (LAMA1) and nidogen 1 precursor (NID1). NID1 is a glycoprotein that displays increased expression from wk 2 to 10 in the postnatal prefrontal cortex [49] and has been shown to play a role in cell adhesion [50]. Due to its high expression and membrane localization, NID1 may be a useful marker for GPCs. Finally, the OPC stage produced a total of 24 potential markers, including several crystallin proteins (CRYBA1, CRYBB1, CRYBB3, CRYBA4, CRYBA2, CRYAA, CRYAB, CRYGS), galactein-1 (LGALS1), HtrA serine peptidase 1 (HTRA1) and FABP4.

In addition to marker expression, information obtained in these analyses from human cells has potential clinical

implications in future translational research involving the OL lineage. For instance, several laboratories have identified changes in the gene and protein expression in schizophrenic [51] and multiple sclerosis patients [40]. While the role of OLs injury in multiple sclerosis is well established [52] numerous lines of evidence implicate the role OL injury in the loss of connectivity associated with schizophrenia [41, 51]. These studies have included comparisons of both transcriptome and proteomic alterations that have identified several OL-related proteins in the progression of disease that were also found here including CNP, TF, QK1 and GSN [41, 51]. Thus, understanding the markers of human OL development will help toward understanding the pathology of OL-associated diseases.

For instance, in OL-associated diseases or injuries, the sensitivity or vulnerability of OLs to oxidative stress and glutamate-related excitotoxicity has been correlated to the underlying pathology (reviewed in [42]). These studies have focused on the role of proteins involved with apoptosis and glutathione metabolism for OPC and OL survival. This is consistent with our proteomic analyses, which reveal higher levels of SOD and Catalase expression in OPCs compared to ESCs. While the expression of many proteins associated with glutathione metabolism was also detected in our study, their levels of expression did not change during differentiation except for microsomal glutathione *S*-transferase 1, which revealed decreased expression during OPC differentiation.

In summary, the results from our study show the most comprehensive picture of the oligodendroglial proteome and demonstrates how next generation proteomics can be used to identify low abundant molecules at deep low levels. To name a few such examples, several low-level transcription regulators (LIN28, SOX2, TRIM28, PODXL, POU5F1, STAT3, SALL4), many members of protein complexes (proteasome complex, AP1, AP2 and AP3 protein complexes) and proteins involved in stem cell regulatory network (BMP1, WINT5A) were identified and in many cases quantifiable. By utilizing a quantitative proteomics approach, we were able to rigorously characterize the developmental proteomic expression profile of OPC differentiation from human ES cells. We identified several novel potential markers of NPCs, GPCs and OPCs, in addition to many known and/or putative proteins associated with OL lineage cells. Further exploration of these proteins within the OL lineage is likely to yield novel therapies for diagnosing and treating many OL-associated or demyelinating conditions by enhancing the differentiation of OL lineage cells and ultimately the production of myelin.

All the peptides and corresponding protein data found in this study have been deposited in Human Proteinpedia [53] (www.humanproteinpedia.org, identification number HuPA_00671) to facilitate the dissemination of this data set.

This work was partly supported by grants from the Maryland Stem Cell Research Fund, State of Maryland to A.H.A. (2009-MSCRFII-0091-00) and to Raghothama Chaerkady (2011-MSCRFE-0172-00), and grants to A.P. from the High End Instrumentation Program of the National Institutes of Health (S10RR023025) and a NIH roadmap grant for Technology Centers of Networks and Pathways (U54RR020839). We thank the Department of Biotechnology of the Government of India for research support to the Institute of Bioinformatics, Bangalore. We thank Cyndi Liu for cell culture assistance.

Conflict of interest statement: B.D. is an employee of Thermo Fisher Scientific. All other authors have declared no conflict of interest.

5 References

[1] Rossi, S. L., Keirstead, H. S., Stem cells and spinal cord regeneration. *Curr. Opin. Biotechnol.* 2009, *20*, 552–562.

[2] Kerr, D. A., Llado, J., Shamblott, M. J., Maragakis, N. J. et al., Human embryonic germ cell derivatives facilitate motor recovery of rats with diffuse motor neuron injury. *J. Neurosci.* 2003, *23*, 5131–5140.

[3] Rajasekharan, S., Intracellular signaling mechanisms directing oligodendrocyte precursor cell migration. *J. Neurosci.* 2008, *28*, 13365–13367.

[4] Gobert, R. P., Joubert, L., Curchod, M. L., Salvat, C. et al., Convergent functional genomics of oligodendrocyte differentiation identifies multiple autoinhibitory signaling circuits. *Mol. Cell Biol.* 2009, *29*, 1538–1553.

[5] Wang, Z., Colognato, H., Ffrench-Constant, C., Contrasting effects of mitogenic growth factors on myelination in neuron-oligodendrocyte co-cultures. *Glia* 2007, *55*, 537–545.

[6] Calver, A. R., Hall, A. C., Yu, W. P., Walsh, F. S. et al., Oligodendrocyte population dynamics and the role of PDGF in vivo. *Neuron* 1998, *20*, 869–882.

[7] Woodruff, R. H., Fruttiger, M., Richardson, W. D., Franklin, R. J., Platelet-derived growth factor regulates oligodendrocyte progenitor numbers in adult CNS and their response following CNS demyelination. *Mol. Cell Neurosci.* 2004, *25*, 252–262.

[8] Winkler, S., Stahl, R. C., Carey, D. J., Bansal, R., Syndecan-3 and perlecan are differentially expressed by progenitors and mature oligodendrocytes and accumulate in the extracellular matrix. *J. Neurosci. Res.* 2002, *69*, 477–487.

[9] Gallo, V., Zhou, J. M., McBain, C. J., Wright, P., et al., Oligodendrocyte progenitor cell proliferation and lineage progression are regulated by glutamate receptor-mediated K+channel block. *J. Neurosci.* 1996, *16*, 2659–2670.

[10] Carson, M. J., Behringer, R. R., Brinster, R. L., McMorris, F. A., Insulin-like growth factor I increases brain growth and central nervous system myelination in transgenic mice. *Neuron* 1993, *10*, 729–740.

[11] Barres, B. A., Lazar, M. A., Raff, M. C., A novel role for thyroid hormone, glucocorticoids and retinoic acid in timing oligodendrocyte development. *Development* 1994, *120*, 1097–1108.

[12] Canoll, P. D., Musacchio, J. M., Hardy, R., Reynolds, R. et al., GGF/neuregulin is a neuronal signal that promotes the proliferation and survival and inhibits the differentiation of oligodendrocyte progenitors. *Neuron* 1996, *17*, 229–243.

[13] McKinnon, R. D., Piras, G., Ida, J. A., Jr., Dubois-Dalcq, M., A role for TGF-beta in oligodendrocyte differentiation. *J. Cell Biol.* 1993, *121*, 1397–1407.

[14] Mayer, M., Bogler, O., Noble, M., The inhibition of oligodendrocytic differentiation of O-2A progenitors caused by basic fibroblast growth factor is overridden by astrocytes. *Glia* 1993, *8*, 12–19.

[15] Emery, B., Agalliu, D., Cahoy, J. D., Watkins, T. A. et al., Myelin gene regulatory factor is a critical transcriptional regulator required for CNS myelination. *Cell* 2009, *138*, 172–185.

[16] Wegner, M., A matter of identity: transcriptional control in oligodendrocytes. *J. Mol. Neurosci.* 2008, *35*, 3–12.

[17] Fancy, S. P., Baranzini, S. E., Zhao, C., Yuk, D. I. et al., Dysregulation of the Wnt pathway inhibits timely myelination and remyelination in the mammalian CNS. *Genes Dev.* 2009, *23*, 1571–1585.

[18] Ye, F., Chen, Y., Hoang, T., Montgomery, R. L. et al., HDAC1 and HDAC2 regulate oligodendrocyte differentiation by disrupting the beta-catenin-TCF interaction. *Nat. Neurosci.* 2009, *12*, 829–838.

[19] Chaerkady, R., Kerr, C. L., Marimuthu, A., Kelkar, D. S. et al., Temporal analysis of neural differentiation using quantitative proteomics. *J. Proteome Res.* 2009, *8*, 1315–1326.

[20] Irizarry, R. A., Ladd-Acosta, C., Wen, B., Wu, Z. et al., The human colon cancer methylome shows similar hypo- and hypermethylation at conserved tissue-specific CpG island shores. *Nat. Genet.* 2009, *41*, 178–186.

[21] Kerr, C. L., Letzen, B. S., Hill, C. M., Agrawal, G. et al., Efficient differentiation of human embryonic stem cells into oligodendrocyte progenitors for application in a rat contusion model of spinal cord injury. *Int. J. Neurosci.* 2010, *120*, 305–313.

[22] Letzen, B. S., Liu, C., Thakor, N. V., Gearhart, J. D. et al., MicroRNA expression profiling of oligodendrocyte differentiation from human embryonic stem cells. *PLoS ONE* 2010, *5*, e10480.

[23] Chaerkady, R., Kerr, C. L., Kandasamy, K., Marimuthu, A. et al., Comparative proteomics of human embryonic stem cells and embryonal carcinoma cells. *Proteomics* 2010, *10*, 1359–1373.

[24] Chaerkady, R., Kerr, C. L., Kandasamy, K., Marimuthu, A. et al., Comparative proteomics of human embryonic stem cells and embryonal carcinoma cells. *Proteomics* 2010, *10*, 1359–1373.

[25] Da Wei Huang, B., Lempicki, R., Systematic and integrative analysis of large gene lists using DAVID bioinformatics resources. *Nat. Protoc.* 2008, *4*, 44–57.

[26] Dennis, G., Jr., Sherman, B., Hosack, D., Yang, J. et al., DAVID: database for annotation, visualization, and integrated discovery. *Genome Biol.* 2003, *4*, P3.

[27] Huang da, W., Sherman, B. T., Lempicki, R. A., Systematic and integrative analysis of large gene lists using DAVID bioinformatics resources. *Nat. Protoc.* 2009, *4*, 44–57.

[28] Palser, A., Norman, A., Saffell, J., Reynolds, R., Neural cell adhesion molecule stimulates survival of premyelinating oligodendrocytes via the fibroblast growth factor receptor. *J. Neurosci. Res.* 2009, *87*, 3356–3368.

[29] Korshunova, I., Caroni, P., Kolkova, K., Berezin, V. et al., Characterization of BASP1-mediated neurite outgrowth. *J. Neurosci. Res.* 2008, *86*, 2201–2213.

[30] van Noort, J. M., Bsibsi, M., Gerritsen, W. H., van der Valk, P. et al., Alphab-crystallin is a target for adaptive immune responses and a trigger of innate responses in preactive multiple sclerosis lesions. *J. Neurpathol. Exp. Neurol.* 2010, *69*, 694–703.

[31] Ousman, S., Tomooka, B., Van Noort, J., Wawrousek, E. et al., Protective and therapeutic role for α B-crystallin in autoimmune demyelination. *Nature* 2007, *448*, 474–479.

[32] Musse, A., Gao, W., Homchaudhuri, L., Boggs, J., Harauz, G., Myelin basic protein as a ''PI (4, 5) P2-Modulin'': a new biological function for a major central nervous system protein. *Biochemistry* 2008, *47*, 10372–10382.

[33] Bhat, N., Zhang, P., Bhat, A., The expression of myristoylated alanine-rich C-kinase substrate in oligodendrocytes is developmentally regulated. *Dev. Neurosci.* 1995, *17*, 256–263.

[34] See, J., Mamontov, P., Ahn, K., Wine-Lee, L. et al., BMP signaling mutant mice exhibit glial cell maturation defects. *Mol. Cell Neurosci.* 2007, *35*, 171–182.

[35] Nichols, J., Chambers, I., Taga, T., Smith, A., Physiological rationale for responsiveness of mouse embryonic stem cells to gp130 cytokines. *Development* 2001, *128*, 2333–2339.

[36] Azzedine, H., Bolino, A., Taieb, T., Birouk, N. et al., Mutations in MTMR13, a new pseudophosphatase homologue of MTMR2 and Sbf1, in two families with an autosomal recessive demyelinating form of Charcot-Marie-Tooth disease associated with early-onset glaucoma. *Am. J. Human Genet.* 2003, *72*, 1141–1153.

[37] Espinosa-Jeffrey, A., Wakeman, D., Kim, S., Snyder, E., de Vellis, J., Culture system for rodent and human oligodendrocyte specification, lineage progression, and maturation. *Curr. Protoc. Stem Cell Biol.* 2009. Chapter 2 Unit 20.4.

[38] Scolding, N., Morgan, B., Compston, D., The expression of complement regulatory proteins by adult human oligodendrocytes. *J. Neuroimmunol.* 1998, *84*, 69–75.

[39] Pasinetti, G., Johnson, S., Oda, T., Rozovsky, I., Finch, C., Clusterin (SGP-2): a multifunctional glycoprotein with regional expression in astrocytes and neurons of the adult rat brain. *J. Comp. Neurol.* 2004, *339*, 387–400.

[40] Artemiadis, A. K., Anagnostouli, M. C., Apoptosis of oligodendrocytes and post-translational modifications of myelin basic protein in multiple sclerosis: possible role for the early stages of multiple sclerosis. *Eur. Neurol.* 2010, *63*, 65–72.

[41] Davis, K. L., Stewart, D. G., Friedman, J. I., Buchsbaum, M. et al., White matter changes in schizophrenia: evidence for

myelin-related dysfunction. *Arch. Gen. Psychiatry* 2003, *60*, 443–456.

[42] Butts, B. D., Houde, C., Mehmet, H., Maturation-dependent sensitivity of oligodendrocyte lineage cells to apoptosis: implications for normal development and disease. *Cell Death Differ.* 2008, *15*, 1178–1186.

[43] Emery, B., Regulation of oligodendrocyte differentiation and myelination. *Science* 2010, *330*, 779–782.

[44] Lin, G., Mela, A., Guilfoyle, E., Goldman, J., Neonatal and adult O4+oligodendrocyte lineage cells display different growth factor responses and different gene expression patterns. *J. Neurosci. Res.* 2009, *87*, 3390.

[45] Hu, J., Fu, S., Zhang, K., Li, Y. et al., Differential gene expression in neural stem cells and oligodendrocyte precursor cells: a cDNA microarray analysis. *J. Neurosci. Res.* 2004, *78*, 637–646.

[46] Kippert, A., Trajkovic, K., Fitzner, D., Opitz, L., Simons, M., Identification of Tmem 10/Opalin as a novel marker for oligodendrocytes using gene expression profiling. *BMC Neurosci.* 2008, *9*, 40.

[47] Back, S., Tuohy, T., Chen, H., Wallingford, N. et al., Hyaluronan accumulates in demyelinated lesions and inhibits oligodendrocyte progenitor maturation. *Nat. Med.* 2005, *11*, 966–972.

[48] Deshpande, A., Dai, Y., Kim, Y., Kim, J. et al., Cdk2ap1 is required for epigenetic silencing of Oct4 during murine embryonic stem cell differentiation. *J. Biol. Chem.* 2009, *284*, 6043.

[49] Semeralul, M., Boutros, P., Likhodi, O., Okey, A. et al., Microarray analysis of the developing cortex. *J. Neurobiol.* 2006, *66*, 1646–1658.

[50] Ulazzi, L., Sabbioni, S., Miotto, E., Veronese, A. et al., Nidogen 1 and 2 gene promoters are aberrantly methylated in human gastrointestinal cancer. *Mol. Cancer* 2007, *6*, 17.

[51] Martins-de-Souza, D., Proteome and transcriptome analysis suggests oligodendrocyte dysfunction in schizophrenia. *J. Psychiatr. Res.* 2010, *44*, 149–156.

[52] Zeis, T., Schaeren-Wiemers, N., Lame ducks or fierce creatures? The role of oligodendrocytes in multiple sclerosis. *J. Mol. Neurosci.* 2008, *35*, 91–100.

[53] Kandasamy, K., Keerthikumar, S., Goel, R., Mathivanan, S. et al., Human Proteinpedia: a unified discovery resource for proteomics research. *Nucleic Acids Res.* 2009, *37*, D773–D781.

